A Ligation DNAzyme-Driven Catalytic Hairpin Assembly Strategy for miRNA Detection

Hongbo Zhang[a], Yugang Xiao[a], Zhuoer Zeng[b], Di Zhang[c], Zhirui Song[a], Xiaoke Wu[a], Qubo Zhu[a*]

[a] Xiangya School of Pharmaceutical Sciences, Central South University, Changsha, Hunan, China

[b] School of Engineering, University of Glasgow, Glasgow, United Kingdom

[c] Precision Diagnosis Center, The Third Xiangya Hospital, Central South University, Changsha 410013, P.R. China.

E-mail: qubozhu@csu.edu.cn

Fig. S1

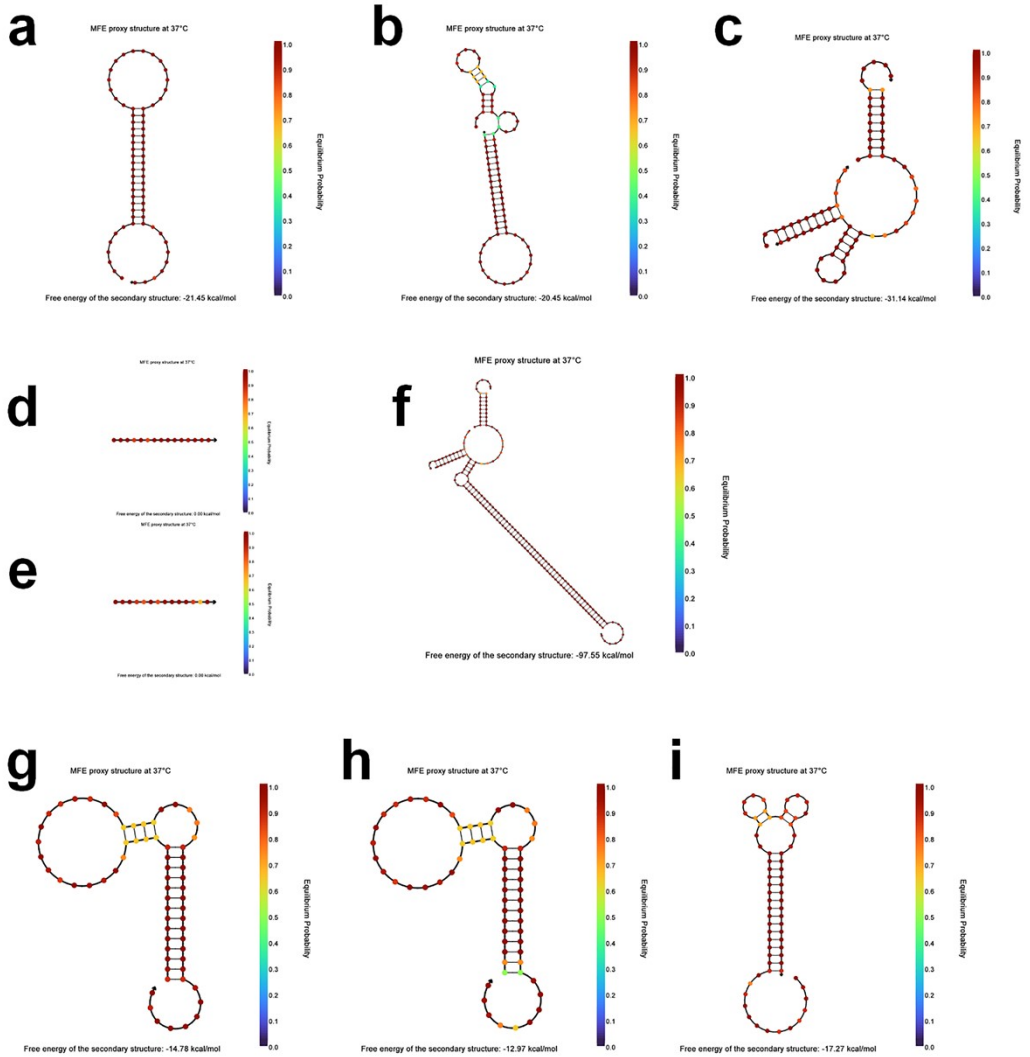

Fig. S1. **NUPACK-predicted secondary structures of oligonucleotide components used in the LiD-CHA system**. (a) H1. (b) H2. (c) E47-A in the presence of substrates S1 and S2. (d) S1. (e) S2. (f) Mixture of H1, H2, S1, and S2. (g) H0-1. (h) H0-2. (i) H0-3.

Fig. S2

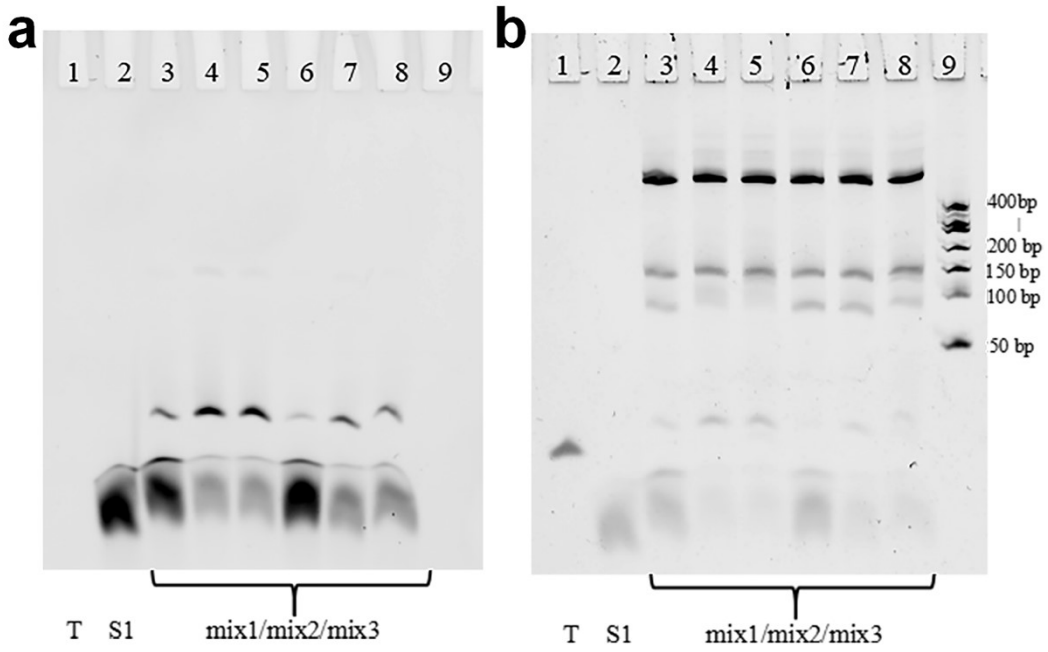

Fig. S2 A 20% denaturing PAGE analysis of the ligation activity of the LiD-CHA system. (a) Unstained gel image. (b) SYBR Green I–stained gel image. Lane 1, trigger (T); lane 2, FAM-labeled S1; lanes 3–5, reaction mixtures (mix-1 to mix-3) incubated at room temperature overnight; lanes 6–8, reaction mixtures (mix-1 to mix-3) incubated at room temperature for 4 h; lane 9, DNA marker. Mix-1 and mix-2 contain 1 μM and 2 μM of the CHA-generated H1-H2 complex, respectively, together with FAM-labeled S1 and S2. Mix-3 contains T, H1, H2, FAM-labeled S1, and S2.

Fig. S3

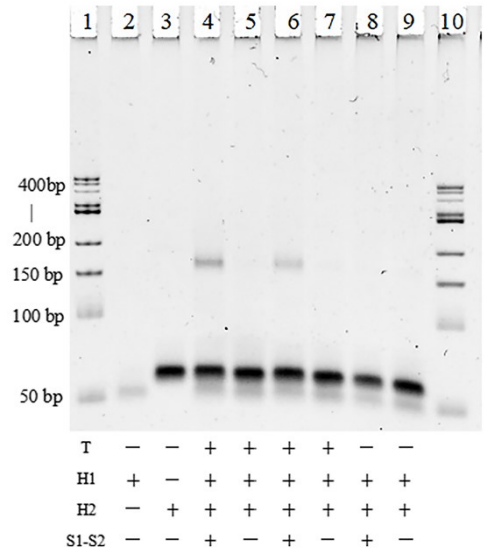

Fig. S3. **Evaluation of background interference from substrates S1 and S2 in the LiD-CHA system.** A 12% native PAGE analysis of different reaction mixtures. Lane 1, DNA marker; lane 2, H1; lane 3, H2; lane 4, 10 nM trigger (T) + H1 + H2 + S1 + S2; lane 5, 10 nM T + H1 + H2; lane 6, 5 nM T + H1 + H2 + S1 + S2; lane 7, 5 nM T + H1 + H2; lane 8, H1 + H2 + S1 + S2; lane 9, H1 + H2; lane 10, DNA marker.

Fig. S4

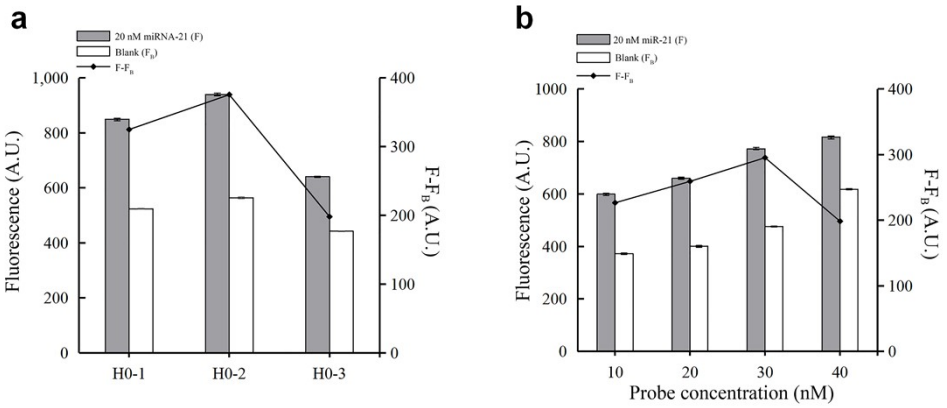

Fig. S4. Optimization of the H0 hairpin probe for miRNA-21 recognition in the LiD-CHA system. (a) Fluorescence responses of LiD-CHA systems constructed with different H0 sequences (H0-1, H0-2, and H0-3) in the presence of 20 nM miRNA-21 and in the absence of the target (blank). (b) Effect of H0 probe concentration on the fluorescence response of the LiD-CHA system in the presence of 20 nM miRNA-21 and under blank conditions. Gray bars represent fluorescence signals obtained in the presence of miRNA-21 (F), white bars represent background fluorescence signals (F_B), and black lines correspond to the net fluorescence intensity ($F-F_B$). Error bars represent the standard deviation of three independent experiments.

Fig. S5

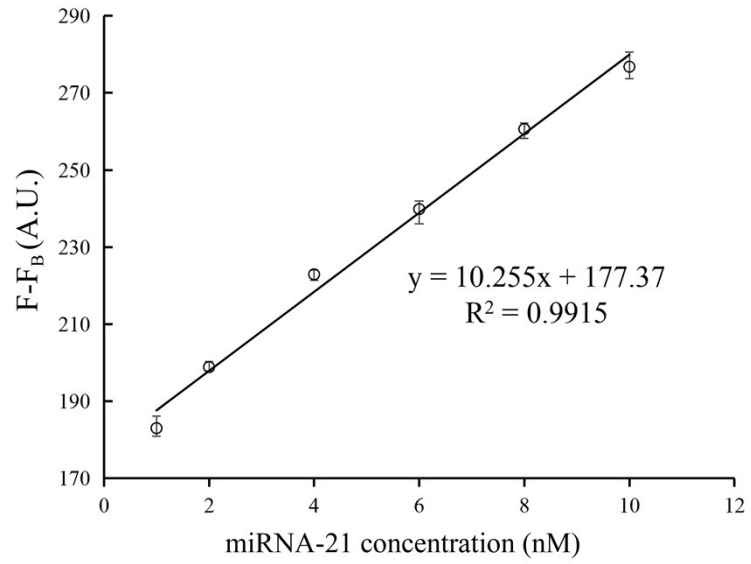

Fig. S5 Calibration curve of fluorescence response for the LiD-CHA system in the concentration range of 1-10 nM. Net fluorescence intensity ($F-F_B$) plotted as a function of miRNA-21 concentration. The solid line represents the linear fitting of the experimental data. Error bars represent the standard deviation of three independent experiments.

Fig. S6

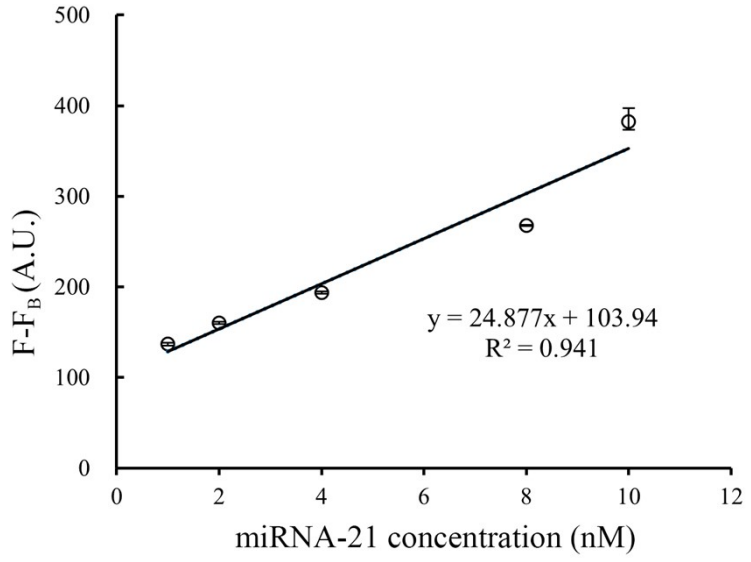

Fig. S6. Calibration curve of fluorescence response for the conventional CHA system lacking S1 and S2. Net fluorescence intensity ($F-F_B$) plotted as a function of miRNA-21 concentration. The solid line represents the linear fitting of the experimental data. Error bars represent the standard deviation of three independent experiments.

Fig. S7

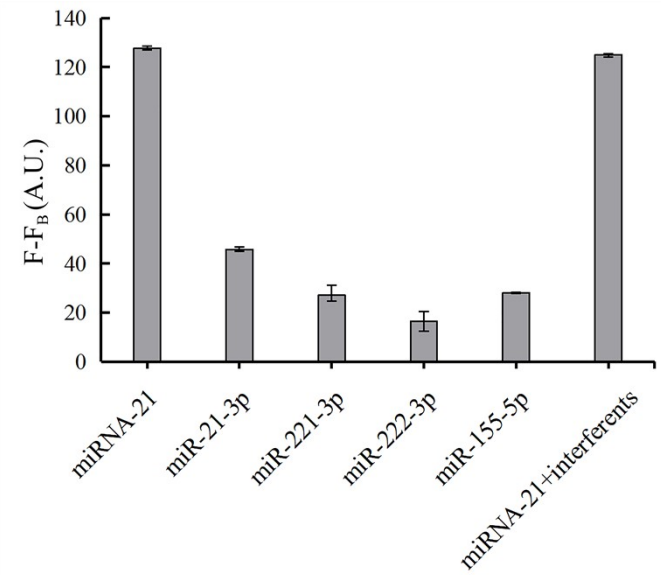

Fig. S7 Specificity and anti-interference evaluation of the LiD-CHA system toward representative non-target miRNAs. Net fluorescence intensities (F-F_B) were measured for miRNA-21, miR-21-3p, miR-221-3p, miR-222-3p, miR-155-5p, and a mixed sample containing miRNA-21 together with miR-21-3p, miR-221-3p, miR-222-3p, and miR-155-5p. Error bars represent the standard deviation of three independent experiments.

Fig. S8

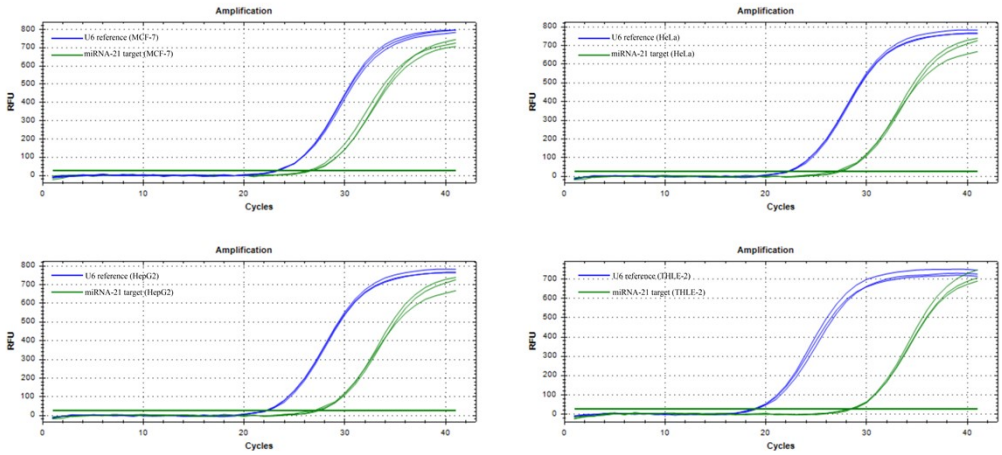

Fi. S8 Raw RT-qPCR amplification curves of miRNA-21 in different cell lines. Amplification curves obtained from RT-qPCR analysis of miRNA-21 in MCF-7, HeLa, HepG2 and THLE-2 cells. Blue curves represent the amplification of the internal reference gene U6, while green curves represent the amplification of miRNA-21.

Fig. S9

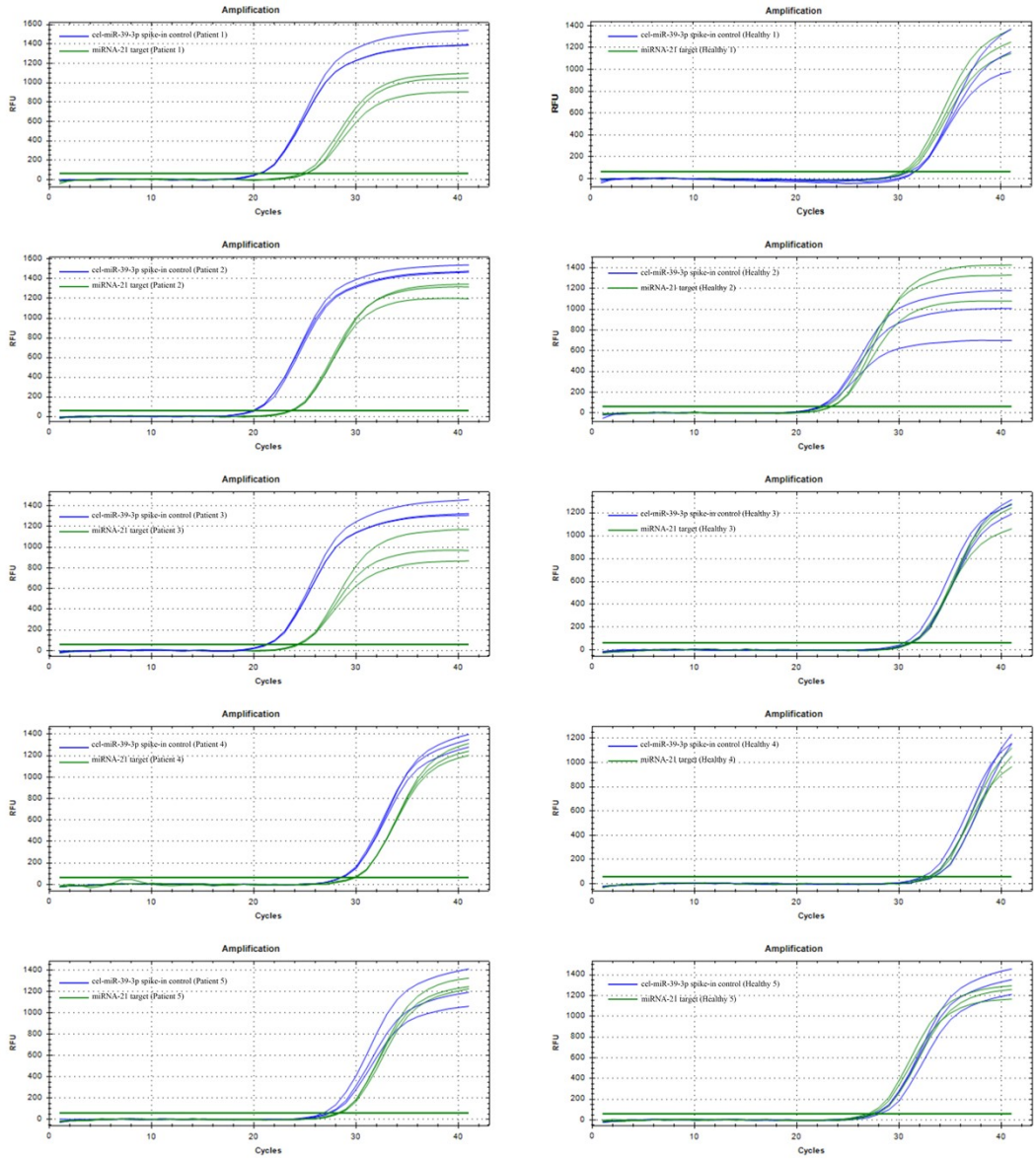

Fig. S9 Raw RT-qPCR amplification curves of miRNA-21 in blood samples from cancer patients and healthy volunteers. Amplification curves obtained from RT-qPCR analysis of miRNA-21 in blood samples from cancer patients and healthy volunteers. Blue curves represent the amplification of the spike-in control cel-miR-39-3p, while green curves represent the amplification of miRNA-21.

Table S1. Recovery of miRNA-21 in spiked samples using the LiD-CHA system. (n=3)

Spiked (pM)	Found (pM)	Recovery (%)	RSD (%)
80	78.7 ± 1.1	98.4	1.3
50	49.6 ± 0.3	99.2	0.7
30	31.6 ± 0.2	105.2	0.6
15	15.5 ± 0.4	103.4	2.3